

Lyman Break Galaxies at $z \sim 5$: Rest-frame UV Spectra

II *

Masataka ANDO, Kouji OHTA

*Department of Astronomy, Kyoto University,
Oiwake-cho, Kirashirakawa, Sakyo-ku, Kyoto, 606-8502
andoh@kusastro.kyoto-u.ac.jp, ohta@kusastro.kyoto-u.ac.jp*

Ikuru IWATA

*Okayama Astrophysical Observatory, National Astronomical Observatory of Japan,
Kamogata, Okayama 719-0232
iwata@oao.nao.ac.jp*

Masayuki AKIYAMA, Kentaro AOKI, and Naoyuki TAMURA

*Subaru Telescope, National Astronomical Observatory of Japan,
650 North A'ohoku Place, Hilo, Hawaii 96720, USA
akiyama@subaru.naoj.org, kaoki@subaru.naoj.org, naoyuki@subaru.naoj.org*

(Received 2007 January 29; accepted 2007 May 7)

Abstract

We present the results of spectroscopy of Lyman Break Galaxies (LBGs) at $z \sim 5$ in the J0053+1234 field with the Faint Object Camera and Spectrograph on the Subaru telescope. Among 5 bright candidates with $z' < 25.0$ mag, 2 objects are confirmed to be at $z \sim 5$ from their Ly α emission and the continuum depression shortward of Ly α . The EWs of Ly α emission of the 2 LBGs are not so strong to be detected as Ly α emitters, and one of them shows strong low-ionized interstellar (LIS) metal absorption lines. Two faint objects with $z' \geq 25.0$ mag are also confirmed to be at $z \sim 5$, and their spectra show strong Ly α emission in contrast to the bright ones. These results suggest a deficiency of strong Ly α emission in bright LBGs at $z \sim 5$, which has been discussed in our previous paper. Combined with our previous spectra of LBGs at $z \sim 5$ obtained around the Hubble Deep Field-North (HDF-N), we made a composite spectrum of UV luminous ($M_{1400} \leq -21.5$ mag) LBGs at $z \sim 5$. The resultant spectrum shows a weak Ly α emission and strong LIS absorptions which suggests that the bright LBGs at $z \sim 5$ have chemically evolved at least to ~ 0.1 solar metallicity. For a part of our sample in the HDF-N region, we obtained near-to-mid infrared data, which constraint stellar masses of these objects. With the stellar mass and the metallicity estimated from LIS absorptions, the metallicities of the LBGs at $z \sim 5$ tend to be lower than those of the galaxies with the same stellar mass at $z \lesssim 2$,

although the uncertainty is very large.

Key words: galaxies: evolution — galaxies: formation — galaxies: high-redshift

1. Introduction

Spectroscopic studies of high-redshift ($z > 2 \sim 3$) galaxies have been advanced recently. One of the largest spectroscopic samples of high- z galaxies is obtained by follow-up spectroscopy for Lyman Break galaxies (LBGs: e.g., Steidel et al. 2003) which are selected by using multi-band photometric data. So far, about a thousand of optical spectra have been obtained each for LBGs at $z \sim 3$ (e.g., Shapley et al. 2003) and star-forming galaxies at $z \sim 2$ (BM/BX objects: e.g., Steidel et al. 2004). Intensive spectroscopic studies based on magnitude-limited samples have also identified several hundreds of galaxies at $z \sim 2 - 4$ (e.g. FORS Deep Field (FDF) survey: Noll et al. 2004, VIRMOS-VLT Deep Survey: Le Fèvre et al. 2005).

These studies revealed spectroscopic features of galaxies at $z \sim 2 - 3$ in their rest-frame UV wavelength region, and deepened our understanding of their nature. Shapley et al. (2003) found relations between the strength of the Ly α equivalent width (EW) and other spectroscopic features (e.g., EW of the low-ionized interstellar (LIS) metal absorption lines, UV continuum slope, velocity offset between Ly α and LIS absorptions) for the LBGs at $z \sim 3$, which sheds light on properties of an interstellar matter such as a gas outflow, a velocity dispersion of the gas, and a covering fraction of dust. With a part of FDF data, Mehlert et al. (2002) found that EW of the CIV $\lambda\lambda 1548, 1550$ absorption line decreases from $z \sim 1.4$ to ~ 3.4 . The decrease in the EW of CIV is confirmed with the full sample of FDF, and it seems to continue to $z \sim 4$ (Noll et al. 2004). Since the EW of CIV is an indicator of the metallicity in local starburst galaxies (e.g., Heckman et al. 1998), the result suggests a chemical evolution of galaxies in this redshift range (Mehlert et al. 2002), although the correlation between the metallicity and the EW of CIV has not been calibrated at high-redshift and thus is not ensured. Near-infrared (NIR) spectra of galaxies at $z \sim 2 - 3$ have also been obtained and give information about kinematics and metallicity of the galaxies. The velocity offset between nebula emission lines and interstellar absorption lines is generally seen in the LBGs, suggesting the presence of the gas outflow (e.g., Pettini et al. 2001). From the emissions lines, gas metallicity in the galaxies can be derived by using metallicity estimators (the R_{23} and the N2 index); for example, Teplitz et al. (2000), Kobulnicky & Koo (2000), and Pettini et al. (2001) derived metallicity of LBGs at $z \sim 3$ which ranges typically from 0.1–0.9 solar value. Shapley et al. (2004) showed that majority of the seven NIR bright ($K_{s,Vega} \leq 20$ mag) BX galaxies have near the solar metallicity, and Erb et al. (2006) investigated the extended sample mainly with $K_{s,Vega} < 21.5$ mag and found the median

* Based on data collected at Subaru Telescope, which is operated by the National Astronomical Observatory of Japan.

metallicity of 87 galaxies at $z \sim 2$ to be about 0.5–0.6 solar value.

Recently, surveys of galaxies at $z \gtrsim 5$ have been carried out (e.g. Iwata et al. 2003; Lehnert & Bremer 2003; Stanway et al. 2003; Dickinson et al. 2004; Ouchi et al. 2004; Shimasaku et al. 2005; Yan et al. 2005; Bouwens et al. 2006; Yoshida et al. 2006), and challenges of finding galaxies even at $z \sim 7 - 10$ have also started (e.g., Pello et al. 2004; Kneib et al. 2004; Bouwens et al. 2005; Bouwens & Illingworth 2006; Mannucci et al. 2007). However, the progress of optical follow-up spectroscopy for galaxies at $z \gtrsim 4 - 5$ is much slower than that for galaxies at $z = 2 \sim 3$ because objects are getting fainter, and characteristic features of UV spectrum of star-forming galaxies (e.g., Ly α , LIS absorptions) redshift to the wavelength region where night sky emissions are very strong. Although attempts of spectroscopic observations of galaxies at $z \gtrsim 5$ were made (e.g., Spinrad et al. 1998; Dey et al. 1998; Weymann et al. 1998; Lehnert & Bremer 2003; Stanway et al. 2004), most of the galaxies were identified only with a Ly α emission because of the low signal-to-noise ratio of their continuum light.

We also started an optical spectroscopy of LBGs at $z \sim 5$. Targets were selected from our surveys for LBGs at $z \sim 5$ (Iwata et al. 2003, 2007) which consist of the deep and wide V, I_C , and z' -band imaging survey with the Subaru/Suprime-Cam in the two target fields: the region including the Hubble Deep Field-North (the HDF-N region) and the J0053+1234 region. Our survey fields are quite wide (1290 arcmin² in total), and we obtain 228 bright objects with $z'_{AB} < 25.0$ mag ($L \gtrsim L^*$ in UV luminosity function (UVLF) of LBGs at $z \sim 5$). We reported an initial result of the spectroscopy for a part of the objects in the HDF-N region (Ando et al. 2004: hereafter Paper I). Thanks to the object brightness and good observing conditions, we detected continuum features of the LBGs at $z \sim 5$ and identified the galaxies to be at $z \sim 5$ without Ly α emission line. The most striking result was that there is no or a weak ($EW_{\text{rest}} < 10\text{\AA}$) Ly α emission line in 7 bright LBGs identified. Inspired by the result, the deficiency of the strong Ly α emission in the bright LBGs at $z \sim 5$ was investigated by using combined data of Paper I, our new results obtained in the J0053+1234 region, and those from the literature; the deficiency is generally seen in the LBGs at $z \sim 5$ and even at $z \sim 6$ (Ando et al. 2006). If the quenched Ly α emission is due to the dust, this deficiency suggests that bright LBGs have larger amount of dust and higher metallicity than faint ones. This hypothesis suggests that bright LBGs experienced star formation earlier than that of faint ones: differential evolution of the high-redshift galaxies with their luminosity, although there are other possible origins of the deficiency (e.g., a velocity structure in/around the galaxy).

In this paper, we present the data of spectroscopic observation of LBGs at $z \sim 5$ in the J0053+1234 region which were used in our previous paper (Ando et al. 2006). In Section 2, we describe a sample selection, observation, and data reduction. The features of obtained spectra of the LBGs at $z = 4 - 5$ in the J0053+1234 region are shown in Section 3. Combining this result with our previous results (Paper I), we described spectroscopic properties of bright LBGs at $z \sim 5$ and metallicity against stellar mass in the section. Throughout this paper, we adopt

flat Λ cosmology, $\Omega_M = 0.3$, $\Omega_\Lambda = 0.7$, and $H_0 = 70 \text{ km s}^{-1}\text{Mpc}^{-1}$. The magnitude system is based on AB magnitude (Oke & Gunn 1983).

2. Observation and Data Reduction

The photometric sample of LBGs at $z \sim 5$ in the J0053+1234 region was selected based on a deep and wide broad-band (V , I_C , and z') imaging survey by using Subaru/Suprime-Cam (Iye et al. 2004; Miyazaki et al. 2002): a total of 114 (236) candidates with $z' < 25.0$ (25.5) mag in an effective survey area ($\sim 800 \text{ arcmin}^2$). Details of imaging observations and the color selection are described in Iwata et al. (2007). In order to detect continuum and absorption feature, we selected the bright ($z' < 25.0$) LBG candidates at $z \sim 5$ as the main spectroscopic targets. Because the entire survey field was too wide to obtain spectra for the whole sample of these LBG candidates with a limited field of view ($6'\phi$) of the Faint Object Camera and Spectrograph (FOCAS: Kashikawa et al. 2002) on the Subaru telescope and limited observing time, we selected a target MOS field to contain the bright LBGs as many as possible. When a slit of a bright target overlapped with a slit of another bright one, we chose the object with a higher central surface brightness. Finally, we designed one FOCAS mask which covers 5 bright LBGs. The mask also covered 8 fainter ($z' \geq 25.0$ mag) LBGs which are in the gaps of the slits of main targets on the mask.

Spectroscopic observations with the Subaru/FOCAS were made on 2004 September 14 under a clear condition, and a seeing during the observing run was typically $\sim 0.''8$ (FWHM). We used a grism of 300 lines mm^{-1} blazed at 7500 Å and the SO58 order-cut filter (the same setting as Paper I), which gave wavelength coverage from 5800Å to 10000Å (depending on a slit position on the mask) with a pixel scale of 1.34Å. The slit lengths were typically 10'', and the slit widths were fixed to be 0.''8, giving a spectral resolution of $R \sim 700$ which was measured with night sky emission lines. An exposure time of each frame was 0.5 hours, and a total effective exposure time was 6 hours.

The data were reduced by using IRAF¹ with the same manner as Paper I except for the re-subtraction of the night sky emissions. We subtracted bias from object frames by using an overscan region of each frame and averaged bias frame in order to remove the characteristic bias-pattern of FOCAS CCDs. Flat-fielding was made with normalized average of dome-flat images. The wavelength calibration was made by using night-sky emission lines. The RMS error of the wavelength calibration was $\sim 0.7\text{\AA}$. After the sky subtraction, the spectrum of each object was carefully aligned and averaged. Because some objects show too low continuum S/N to subtract sky emission in each frame, we carried out sky subtraction after combining spectra for these objects. Five pixels were binned toward wavelength direction in order to improve

¹ Image Reduction and Analysis Facility, distributed by National Optical Astronomical Observatories, which are operated by the Association of Universities for Research in Astronomy, Inc., under cooperative agreement with the National Science Foundation.

S/N, and one-dimensional spectra were obtained with APALL task of IRAF. Since our objects were faint, we did not fix the aperture width for the extraction but we determined it by eye for each object to trace it well. The flux calibration and the sensitivity correction were made for the final spectra by using standard stars of Wolf1346 and PG0823+546. The correction for the atmospheric A and B bands was also made by tracing those absorption features in the spectra of standard stars. For some of the objects, the sky subtraction was not well achieved due to the low-S/N of the continuum or the presence of the bad column of the CCDs. Thus we re-subtracted the scaled night sky emissions from the one-dimensional spectrum of such objects.

3. Results and Discussions

3.1. Redshift Determination

Among 5 bright targets, we identified 2 objects to be LBGs at $z = 4 - 5$, and the resultant spectra are shown in Figure 1 (No.1: top left, No.2: top right). LBG identifications were mainly made by the presence of the continuum depression shortward of the redshifted Ly α due to the inter-galactic HI absorption and the Ly α emission line near the Ly α depression. In addition, the Ly α emission line of each object shows an asymmetric shape which is considered to be characteristic feature of LBGs and Ly α emitters (LAEs) at high-redshift. Note that emission-like features in the spectrum of object No.1 at $\sim 6300\text{\AA}$ and in the wavelength region longer than 7300\AA are the residuals of the night sky emissions since the sky subtraction was not well achieved due to the bad column in the CCD. For object No.2, we identified some LIS absorption lines (SiII $\lambda 1260$, OI+SiII $\lambda 1303$, and CII $\lambda 1335$) at almost the same redshift of the Ly α which are characteristic features of nearby star-forming galaxies (e.g., Heckman et al. 1998) and LBGs at $z \sim 3 - 5$ (e.g., Steidel et al. 1996; Shapley et al. 2003; Frye et al. 2002; Paper I; Iwata, Inoue & Burgarella 2005), supporting the identifications of high redshift star-forming galaxies. Redshifts of these two bright LBGs were determined from the peak of Ly α emission: 4.797 and 4.267 for object No.1 and No.2, respectively. The error of the redshift determination was ~ 0.005 . The rest of the bright sample were not identified to be at $z \sim 5$ because of their low S/N of the spectra. These objects tend to have lower central surface brightness compared with the confirmed objects.

In addition to the bright targets, we identified 2 objects among faint bonus targets with $z' \geq 25.0$ mag to be LBGs at $z = 4 - 5$. Spectra of them are shown in Figure 1 (No.3: bottom left, and No.4: bottom right). These objects show a strong ($\text{EW}_{\text{obs}} \sim 220\text{\AA}$ and $\sim 420\text{\AA}$ for object No.3 and No.4, respectively) single emission line; peak of the emission corresponds to the redshift of 4.391 and 4.491 for object No.3 and No.4, respectively if this emission is Ly α . A clear asymmetry of the emission line profile and possible continuum depression shortward of the emission are seen in the spectrum of object No.4, which supports this object is really

at $z = 4 - 5$. Because the redshift determinations for these objects were based only on the single emission line, we examine the possibility that they are foreground emission galaxies. For example, if object No.3 (No.4) is an [OII] $\lambda 3727$ emitter at $z = 0.76$ (0.79), they should show the redshifted H β emission line at $\sim 8550(8710)\text{\AA}$ and the [OIII] $\lambda 5007$ emission line at $\sim 8810(8970)\text{\AA}$ with EW_{obs} of $\sim 70(130)\text{\AA}$ and EW_{obs} of $\sim 110(210)\text{\AA}$, respectively by assuming the median of the observed line ratios of star-forming galaxies at $z = 0.3 \sim 1.0$ (0.3 and 0.5, respectively: Kobulnicky & Kewley 2004). As shown in Figure 1, emission-like features are seen around at a part of the expected wavelengths in both spectra. However, these features are residual night-sky emissions, and there is no other significant ($\text{EW}_{\text{obs}} \gtrsim 100\text{\AA}$) emission lines at the expected wavelengths. Thus these strong emissions are considered to be the Ly α emission from LBGs at the target redshift. We can not completely rule out the possibility that they are foreground emission galaxies by only this analysis, because some of the expected lines of foregrounds are in the wavelength region of severe night sky emissions, and the line ratios have wide object-to-object variances (Kobulnicky & Kewley 2004). But the $V - I_C$ colors of these objects (1.98 mag and 1.85 mag) are too red to regard them as star-forming galaxies at $z < 1$; we calculated the SEDs of star-forming galaxies at $z < 1$ by using the population synthesis code PÉGASE version 2 (Fioc & Rocca-Volmerange 1997) with Salpeter IMF (Salpeter 1955) and by assuming constant star formation with an age of 100 Myr, which gives their $V - I_C$ colors in observed-frame of $-0.4 - 0.1$ mag and $0.2 - 0.8$ mag for $E(B - V) = 0.0$ mag and $E(B - V) = 0.4$ mag, respectively with the dust extinction curve by Calzetti et al. (2000). Thus we consider both of the objects are at $z = 4 - 5$.

3.2. Color Selection and Redshift Distribution of LBGs at $z \sim 5$

Figure 2 shows the positions of observed objects in the $V - I_C$ and $I_C - z'$ two-color diagram from the present results and Paper I. Photometric properties of spectroscopically identified LBGs at $z = 4 - 5$ in the J0053+1234 region are summarized in Table 1. Filled circles show LBGs at $z = 4 - 5$ in this study: 2 bright objects as large circles and 2 faint objects as small ones. Filled squares show bright LBGs at $z \sim 5$ in our previous results (Paper I). Open triangles and open-inverse triangles show bright LBG candidates unidentified in our present observation and the previous results, respectively. So far, no bright spectroscopic targets (total of 22 LBG candidates) have been identified as foreground galaxies, though a half of them were not identified due to the low-S/N of their spectra. In order to examine our color selection criteria further, we also show the positions of the Galactic M stars which were identified in our previous observations as filled pentagons in Figure 2. Our selection criteria for LBGs at $z \sim 5$ are reasonable to exclude interlopers, though more large and systematic spectroscopic observations are desirable.

The redshift distribution of the spectroscopically confirmed LBGs at $z \sim 5$ in this study and Paper I is shown in Figure 3. In Figure 3, we plot the expected redshift distribution of our

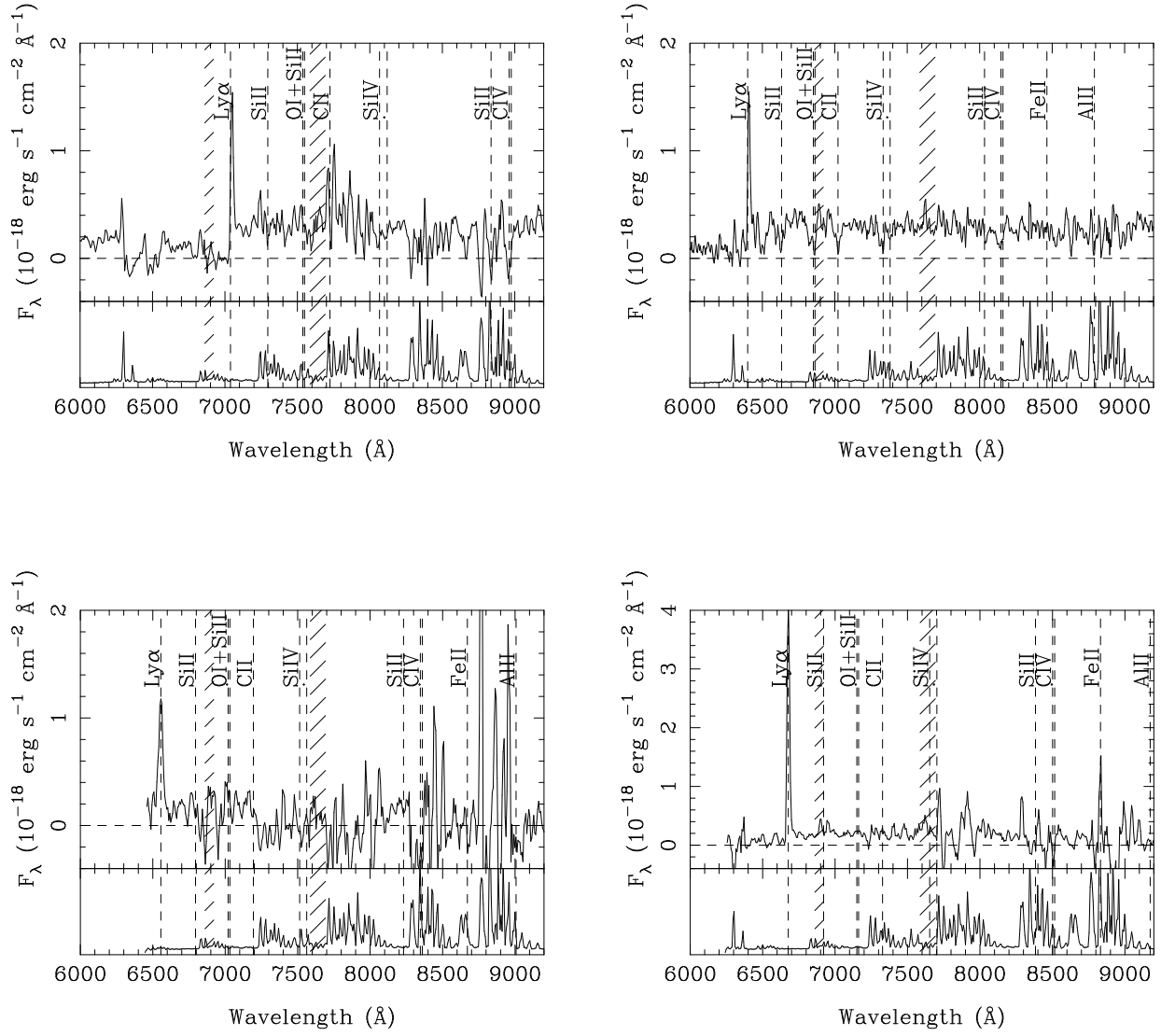


Fig. 1. Spectra of LBGs at $z = 4 - 5$ in the J0053+1234 region. *Top:* Object No.1 (*left*) and No.2 (*right*). *Bottom:* Object No.3 (*left*) and No.4 (*right*). These spectra are smoothed with a boxcar over 3-pixel. Positions of line features seen in LBGs at $z = 3$ and local starburst galaxies (e.g., Shapley et al. 2003; Heckman et al. 1998) are shown with vertical dashed lines. A scaled sky spectrum is shown in a lower part of each panel, and the atmospheric A-band and B-band absorptions are shown as vertical hatched regions.

Table 1. Photometric properties of the LBGs identified to be at $z \sim 5$ in the J0053+1234 region.

No. (ID)	RA(J2000)	DEC(J2000)	z'^*	$V - I_C^\dagger$	$I_C - z'^\dagger$
1 (106426)	00:52:21.34	+12:32:35.3	24.07	2.59	0.23
2 (104115)	00:52:43.27	+12:32:08.2	24.22	1.75	0.16
3 (091813)	00:52:39.88	+12:29:44.1	25.03	1.98	0.06
4 (093014)	00:52:37.37	+12:29:58.7	25.26	>1.85	0.16

* z' magnitude. MAG_AUTO from SExtractor (Bertin and Arnouts 1996) is adopted.

† These values are measured with a $1''.6$ aperture.

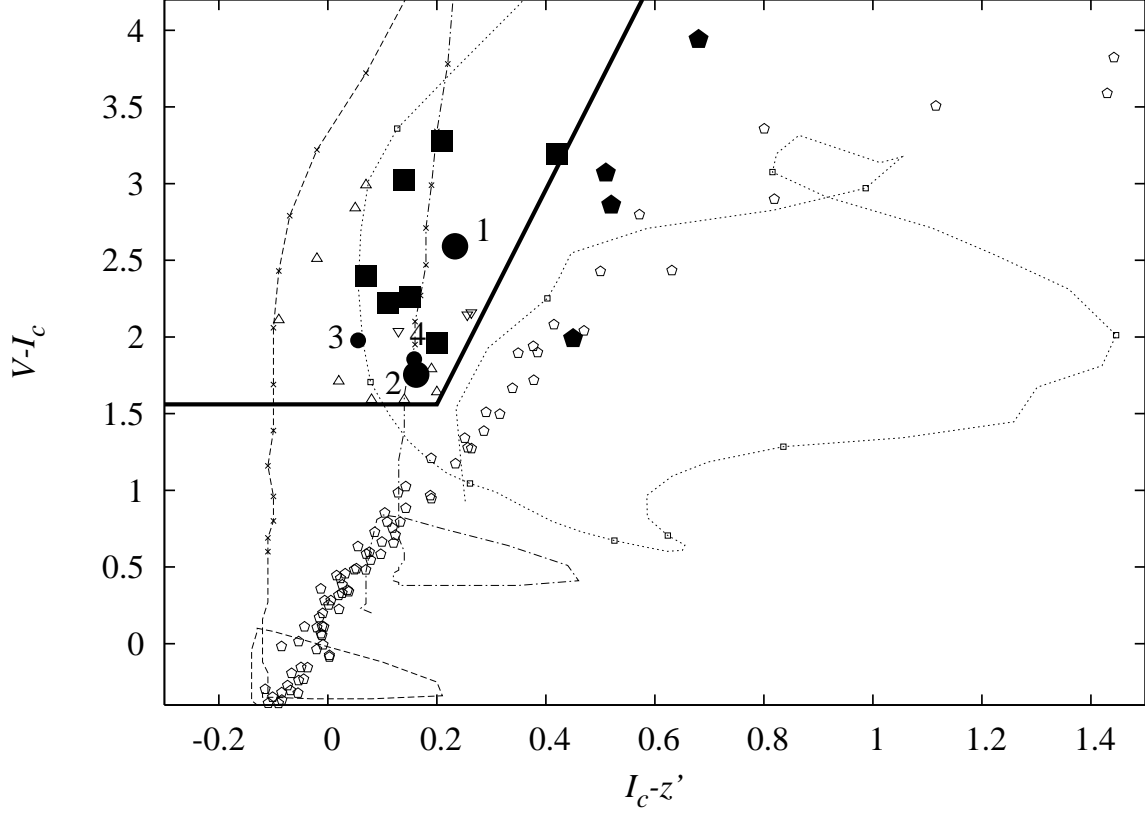


Fig. 2. Positions of identified objects in the $I_C - z'$ and $V - I_C$ two-color diagram. Our color selection criteria for LBGs at $z \sim 5$ (Iwata et al. 2003; 2007) are indicated by thick lines. The objects confirmed to be at $z \sim 5$ in this study are shown as filled circles with each identification number in Table 1. The large circles show 2 bright objects, and small ones show 2 faint objects. Filled squares represent 7 bright LBGs at $z \sim 5$ from Paper I. Open triangles and open-inverse triangles show bright LBG candidates unidentified in our present observation and the previous results (Paper I), respectively. Filled pentagons show objects identified to be foreground objects (Galactic M stars) from Paper I. A dashed (dot-dashed) line represents a color track of a model LBG spectrum with $E(B - V) = 0.0$ mag ($E(B - V) = 0.4$ mag) from Iwata et al. (2007). Small crosses are plotted on the tracks for $z \geq 4.0$ with an interval of 0.1. Model SEDs of LBGs are generated by using the population synthesis code PÉGASE version 2 (Fioc & Rocca-Volmerange 1997) with Salpeter IMF (Salpeter 1955) and by assuming constant star formation with an age of 100 Myr. IGM absorptions at each redshift are calculated by using the analytic formula by Inoue et al. (2005). Calzetti's dust extinction curve (Calzetti et al. 2000) is assumed to make model spectra with $E(B - V) = 0.4$ mag. A dotted line refers to a color track of an elliptical galaxy (Coleman et al. 1980). Small open squares are plotted on the track with a redshift interval of 0.5. Small open pentagons indicate the colors of A0 – M9 stars calculated based on the library by Pickles (1998).

sample of LBGs at $z \sim 5$ as a solid line normalized at $z = 4.7$. The distribution is calculated based on the expected detection rates of the LBGs against the apparent magnitude and the redshift for each survey field (figure 6 by Iwata et al. (2007)). However, the detection rates were derived through simulations in the two-color diagram to estimate the completeness of the photometric catalog, and they do not include the difference of survey volumes for each redshift bin and the difference of the number density at the corresponding UV magnitude for an apparent magnitude at each redshift bin. In order to derive the expected distribution and compare it with the observed redshift distribution of the spectroscopic sample, we corrected the detection rates by adopting the redshift bin size of $\Delta z = 0.2$ and assuming the UVLF of the $z \sim 5$ LBGs (Iwata et al. 2007). Since almost all our spectroscopic sample covers z' magnitude brighter than 25.5 mag, we calculated the expected redshift distributions for three magnitude ranges of 24.0–24.5 mag, 24.5–25.0 mag, and 25.0–25.5 mag for each field, and took the average of them. The distribution of spectroscopically confirmed LBGs is broadly consistent with the expected distribution, but there seems to be a deficiency of the LBGs at around $z \sim 5.0$. Although the sample size is still small and the deficiency may not be significant, this may be due to the presence of severe night sky emission lines which prevent us from detecting the continuum depression and/or Ly α emission. The night sky emission lines whose wavelengths are converted to the redshifts corresponding to the redshift of Ly α are also shown with dotted line in the figure; the sky emission lines are severe for the redshifts larger than 4.9.

As described in section 3.1, spectroscopically identified LBGs in the J0053 region have redshifts of 4.3–4.8 with a mean of 4.5, which is slightly lower than that of the objects in Paper I with redshifts of 4.5–5.2 (mean value of 4.7). In fact, as seen in Figure 2, the 4 objects in the J0053 region are bluer in the $V - I_C$ color than the 7 objects in Paper I. The mean $V - I_C$ color of spectroscopic sample is 2.62 mag and 2.04 mag for the objects in the HDF-N region and in the J0053 region, respectively. However the difference may be due to the variation among small numbers of objects, and we should have more objects with spectroscopic redshifts to examine this point further.

3.3. Spectra of LBGs at $z \sim 5$ in the J0053+1234 region

As shown in Figure 1, spectra of bright LBGs in the J0053+1234 region show Ly α and LIS absorptions (SiII λ 1260, OI+SiII λ 1303, and CII λ 1335) which are typical line features of star-forming galaxies at low and high redshifts. The Ly α EW_{rest}s of object No.1 and No.2 are $14 \pm 3 \text{ \AA}$ and $21 \pm 4 \text{ \AA}$, respectively, and their observed fluxes are $2.5 \times 10^{-17} \text{ erg s}^{-1} \text{ cm}^{-2}$ and $2.4 \times 10^{-17} \text{ erg s}^{-1} \text{ cm}^{-2}$, respectively corresponding to the luminosities of $5.8 \times 10^{42} \text{ erg s}^{-1}$ and $4.3 \times 10^{42} \text{ erg s}^{-1}$, respectively. These values of Ly α do not include absorption component and are not corrected for the IGM absorption. The errors of EW values in this paper include the uncertainty in determination of the continuum level and the RMS error of the continuum. The values of EW of Ly α are larger than the average value of our previous results for 7 bright LBGs

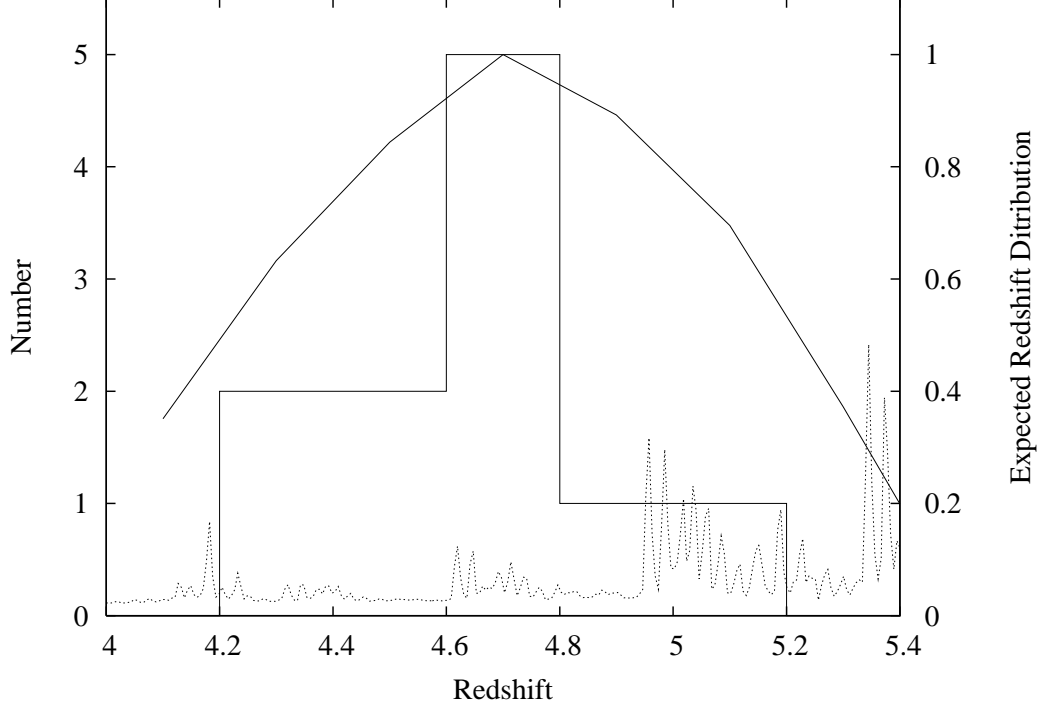


Fig. 3. Redshift distribution of LBGs at $z \sim 5$ from this study and our previous spectroscopic results (Paper I). The night sky emission lines whose wavelengths are converted to the redshifts corresponding to the redshift of $\text{Ly}\alpha$ are also shown with dotted line. Expected redshift distribution normalized at $z = 4.7$ for LBGs at $z \sim 5$ is also plotted as solid line (right vertical axis, see text for the details).

($2.5 \pm 3.7 \text{\AA}$, Paper I), but they are not so large to be detected as definitive LAEs. Typical $\text{Ly}\alpha$ EW_{rest} value for selecting LAEs is $15 \sim 20 \text{\AA}$. In contrast to the result for the bright targets, the $\text{Ly}\alpha$ emissions of the faint LBGs are strong; EW_{rest} of object No.3 and No.4 are $40 \pm 12 \text{\AA}$ and $77 \pm 23 \text{\AA}$, respectively. The observed fluxes of $\text{Ly}\alpha$ are $3.7 \times 10^{-17} \text{ erg s}^{-1} \text{ cm}^{-2}$ and $8.3 \times 10^{-17} \text{ erg s}^{-1} \text{ cm}^{-2}$, respectively corresponding to the luminosities of $7.1 \times 10^{42} \text{ erg s}^{-1}$ and $1.7 \times 10^{43} \text{ erg s}^{-1}$, respectively. We summarize the observed quantities in Table 2.

The bright LBGs at $z \sim 5$ tend to show no or weak $\text{Ly}\alpha$ emission; average EW_{rest} of $\text{Ly}\alpha$ emission of the total of 9 bright LBGs is $\sim 5.8 \pm 7.2 \text{\AA}$, while strong $\text{Ly}\alpha$ emission is seen among the faint LBGs. Because we can not deny the presence of faint LBGs with no or weak $\text{Ly}\alpha$ emission from the current data, these results suggest, at least, a deficiency of strong $\text{Ly}\alpha$ emission in bright LBGs at $z \sim 5$ and might suggest the UV luminosity dependence of the $\text{Ly}\alpha$ emission. Combining with other spectroscopic results from the literature, we found that the deficiency is generally seen in LBGs at $z \sim 5$ and possibly in LBGs at $z \sim 6$ (Ando et al. 2006). The trend is also seen in the galaxies at $z = 4 \sim 6$ (Vanzella et al. 2006; 2007). Possible origins of the deficiency of strong $\text{Ly}\alpha$ emission are discussed by Ando et al. (2006). The deficiency or the UV luminosity dependence of the $\text{Ly}\alpha$ are also seen in the recent results of spectroscopy of LBGs at $z \sim 3$; Shapley et al. (2006) showed that UV luminous ($M_{UV} \sim -21.6 \text{ mag}$) LBGs at

Table 2. Spectroscopic properties of the LBGs identified to be at $z = 4 - 5$ in the J0053+1234 region.

No. (ID)	Redshift*	EW(Ly α) [†]	$F_{\text{Ly}\alpha}$ [‡]	$L_{\text{Ly}\alpha}$ [§]
1 (106426)	4.797	14 ± 3	2.5×10^{-17}	5.8×10^{42}
2 (104115)	4.267	21 ± 4	2.4×10^{-17}	4.3×10^{42}
3 (091813)	4.391	40 ± 12	3.7×10^{-17}	7.1×10^{42}
4 (093014)	4.491	77 ± 23	8.3×10^{-17}	1.7×10^{43}

* Redshifts are determined from the peak of Ly α emission. The error of the redshift determination is ~ 0.005 .

[†] Rest-frame equivalent width of Ly α emission in units of angstroms, not including Ly α absorption. EWs are taken to be positive for emission lines. The error is estimated from the uncertainty of the continuum level determination and the RMS error of the continuum.

[‡] Observed flux of the Ly α emission line in units of $\text{erg s}^{-1} \text{cm}^{-2}$.

[§] Luminosity of the Ly α emission line in units of erg s^{-1} . The slit correction is not applied to the values.

$z \sim 3$ tend to show weaker Ly α emission than the total LBG sample of Shapley et al. (2003). From the re-binned sample of Shapley et al. (2003) with their UV luminosity, Keel (2006) showed that Ly α emission is weaker in the UV luminous ($M_{UV} < -21.0$ mag) LBGs than in fainter LBGs.

For object No.2, we identified LIS absorption lines (SiII $\lambda 1260$, OI+SiII $\lambda 1303$, and CII $\lambda 1335$) at almost the same redshift as the Ly α emission. We also identified SiIV $\lambda 1394$ ($\text{EW}_{\text{rest}} = -2.0 \pm 1.1 \text{ \AA}$)² and CIV $\lambda \lambda 1548, 1551$ ($\text{EW}_{\text{rest}} = -4.9 \pm 1.4 \text{ \AA}$) which are also seen in the spectra of LBGs at ~ 3 (e.g., Shapley et al. 2003). The average EW of the three LIS absorption lines is $-4.2 \pm 1.4 \text{ \AA}$ which is larger than the average value of our previous result ($-2.8 \pm 1.2 \text{ \AA}$: Paper I). The peak of Ly α emission line is redshifted by $280 \pm 210 \text{ km s}^{-1}$ relative to the average of the LIS lines. The peak-to-valley velocity offset which may be related to a large scale gas outflow was also reported in LBGs at $z = 3 \sim 5$ (e.g., Shapley et al. 2003; Frye et al. 2002; Paper I). The offset value of object No.2 is smaller than typical value of LBGs at $z \sim 3$ ($500 - 600 \text{ km s}^{-1}$: Shapley et al. 2003) and that of LBGs at $z \sim 5$ ($\sim 600 \text{ km s}^{-1}$: Paper I). For object No.1, we could not identify significant absorption features due to the residuals of the sky subtraction.

3.4. Composite Spectrum of Luminous LBGs at $z \sim 5$

In order to overcome the low-S/N of each spectrum and investigate typical spectroscopic properties of luminous LBGs at $z \sim 5$, we produced a composite spectrum of 8 LBGs at $z \sim 5$ with $M_{1400} < -21.5$ mag by averaging the spectra obtained in this study and our previous

² We resolved SiIV $\lambda \lambda 1394, 1403$ doublet, but $\lambda 1403$ component was not detected significantly (comparable to 1σ), which is consistent with the observed ratio for LBGs at $z \sim 3$ (Shapley et al. 2003).

study. We derived the absolute UV magnitude from the observed broad band magnitude to the rest-frame 1400Å magnitude assuming a continuum slope β ($f_\lambda \propto \lambda^\beta$) of -1 which is a typical value for LBGs at $z \sim 3$ (Shapley et al. 2003). Before co-adding the spectra, all wavelengths were converted to the rest-frame scale using individual redshifts, and each flux density was normalized at 1250Å.

Figure 4 shows the resultant composite spectrum re-binned to common dispersion of 1\AA pixel^{-1} . Note that the emission-like features except for the Ly α (e.g., around 1275Å, 1425Å) come from the residuals of sky emission lines, and these features are not real. The continuum depression shortward of Ly α by IGM is clearly seen in the composite spectrum. A depression factor D_A (Oke & Korycansky 1982) for the composite spectrum is ~ 0.6 , which agrees with the value of the composite spectrum of LBGs at $z \sim 5$ (Paper I) and the values of QSOs at $z \sim 5$ ($0.1 - 0.7$: e.g., Songaila & Cowie 2002; Songaila 2004). As expected from the previous subsection, EW_{rest} of the Ly α emission is not large ($7.6 \pm 0.8\text{\AA}$), and LIS absorptions are also seen clearly. The EWs of LIS absorptions are $-2.7 \pm 0.36\text{\AA}$, $-1.8 \pm 0.30\text{\AA}$, and $-1.5 \pm 0.29\text{\AA}$ for SiII $\lambda 1260$, OI+SiII $\lambda 1303$, and CII $\lambda 1335$, respectively, which suggests that bright LBGs have been chemically polluted to some extent by metal at $z \sim 5$. The SiIV $\lambda\lambda 1394, 1403$ is also seen in the composite spectrum, and the EW_{rest} s of the SiIV $\lambda 1394$ and the SiIV $\lambda 1403$ are $-2.0 \pm 0.32\text{\AA}$ and $-1.0 \pm 0.26\text{\AA}$, respectively.

The EW_{rest} of Ly α is smaller than that of the composite spectrum of LBGs at $z \sim 3$ (15.1\AA : Shapley et al. 2003); the EW values of LIS absorptions are comparable to or somewhat larger than those of $z \sim 3$ (-1.7\AA , -2.3\AA , and -1.5\AA for SiII $\lambda 1260$, OI+SiII $\lambda 1303$, and CII $\lambda 1335$, respectively). However, the sample luminosity range of our LBGs at $z \sim 5$ ($z' \lesssim 24.8$ mag corresponding to $M_{1400} \lesssim -21.5$ mag) is different from that of LBGs at $z \sim 3$ (mainly $R = 23.5 - 25.5$ mag corresponding to $M_{1400} = -21.8 \sim -19.8$ mag). As described in the previous subsection, we found the deficiency of the strong Ly α emission in luminous LBGs at $z \sim 5$ and pointed out the possible presence of the UV luminosity dependence on the spectroscopic features. Thus we can not discuss the evolution of the spectroscopic feature of LBGs from a simple comparison of the composite spectra.

Although the low S/N around the wavelength range longer than 1400Å does not allow us to estimate metallicity by using 1425 index (e.g., Rix et al. 2003) and CIV index (e.g., Mehlert et al. 2002), we roughly estimate mean metallicity of the 8 luminous LBGs at $z \sim 5$ from LIS absorption lines of the composite spectrum assuming the relation between the mean EW of the three LIS absorptions (SiII $\lambda 1260$, OI+SiII $\lambda 1303$, and CII $\lambda 1335$) and a metallicity calibrated with local star-forming galaxies (Heckman et al. 1998). Since the sample by Heckman et al. (1998) does not cover the low metallicity (i.e., weak LIS absorptions) region, we extrapolated the EW(LIS)-metallicity relation in the middle-to-high ($12 + \log(\text{O}/\text{H}) \gtrsim 8.0$) metallicity region to the lower metallicity region. The estimated metallicity of $12 + \log(\text{O}/\text{H})$ is about 7.6 ± 0.6 corresponding to ~ 0.1 ($0.3 - 0.02$) solar value (8.66: Asplund et al. 2004). The errors come

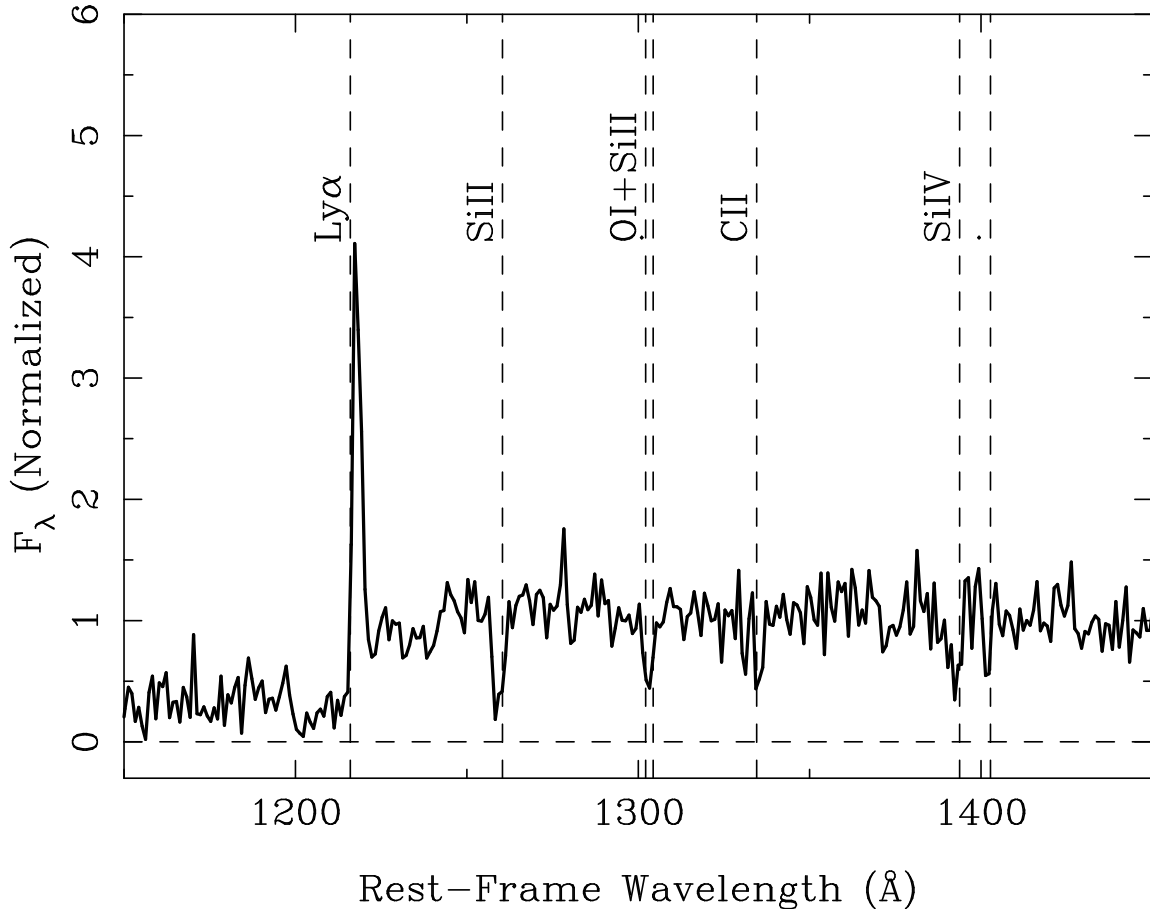


Fig. 4. Composite spectrum of 8 luminous ($M_{1400} < -21.5$ mag) LBGs at $z \sim 5$ from this study and Paper I. Note that most of emission-like features (e.g. around 1275Å, 1425Å) come from the residuals of sky emission lines.

from the uncertainty of the EW measurement as well as that of the empirical relation between the EW(LIS) and metallicity. It should be worth noting that the LIS lines are saturated, and EW(LIS) reflects not only the metallicity but also the velocity structure and covering fraction of the gas (e.g., Heckman et al. 1998; Shapley et al. 2003; Noll et al. 2004). Erb et al. (2006) show a composite rest-frame UV spectrum of objects at $z \sim 2$ with a mean stellar mass of $7 \times 10^{10} M_{\odot}$ and mean metallicity of $12 + \log(\text{O}/\text{H}) \sim 8.55$ derived from N2 index method. The EW(LIS) in the spectrum is $\sim 2 - 3 \text{ \AA}$ corresponding to $12 + \log(\text{O}/\text{H})$ of $\sim 7.6 - 8.2$ if we use the local relation by Heckman et al. (1998). The result suggests that the local EW(LIS)-metallicity relation may systematically underestimate the metallicity of galaxies at high redshift.

3.5. A Hint for Chemical Evolution of massive LBGs at $z \sim 5$?

We derived the individual metallicity for 8 LBGs at $z \sim 5$ with the LIS absorption in this study and Paper I with the same manner mentioned above. For the 3 objects in the HDF-N region among the 8 LBGs, Subaru/CISCO K' band data and Spitzer/IRAC mid-IR data are available, and we can estimate their stellar masses by fitting their rest-frame UV to optical

SEDs to the model SEDs. (Details of NIR and MIR data of our LBGs at $z \sim 5$ will be described elsewhere.) The metallicities ($12+\log(\text{O}/\text{H})$) of 104268 (No.1 of Paper I), 144200 (No.2 of Paper I), and 148198 (No.8 of Paper I) are 7.7 ± 0.8 , 7.7 ± 0.8 , and 8.7 ± 0.9 , respectively. For the stellar mass estimation, we adopted the same manner used in Iwata, Inoue & Burgarella (2005). We used the PÉGASE version 2 population synthesis model (Fioc & Rocca-Volmerange 1997) with Salpeter IMF (Salpeter 1955), constant star formation history, and the Calzetti's dust extinction curve (Calzetti et al. 2000) to make model spectra. IGM absorptions were calculated for the given redshift by using the analytic formula by Inoue et al. (2005). Then the observed SEDs were fit to model SEDs, and the best fit model was obtained by minimizing χ^2 . Resultant stellar masses (best fit value with 68% confidence level) of the objects 104268, 144200, and 148198 are $5.82^{+6.95}_{-3.93} \times 10^{10} M_{\odot}$, $3.33^{+0.94}_{-2.92} \times 10^{10} M_{\odot}$, and $1.33^{+0.67}_{-0.90} \times 10^{11} M_{\odot}$, respectively.

In Figure 5, open circles represent the stellar masses and the metallicities of the three luminous LBGs at $z \sim 5$, and filled circle represents the average value of them. Pluses, diamonds, and triangles show the data for galaxies at $z \sim 0.1$, $z \sim 0.7$ and $z \sim 2$, respectively (Tremonti et al. 2004; Savaglio et al. 2005; Erb et al. 2006), which show the presence of mass-metallicity relation at each redshift and its evolution from $z \sim 2$ to $z \sim 0$ ³. Although the uncertainties are quite large (and may contain some systematics), and our way of metallicity estimation is different from those for galaxies at other redshifts, the metallicities of the LBGs at $z \sim 5$ tend to be lower than those of the galaxies with the same stellar mass at $z \lesssim 2$ ⁴.

We are grateful to the FOCAS team, especially Youichi Ohyama, and the staffs of Subaru telescope for their supports during our observation. We also thank Kiyoto Yabe and Marcin Sawicki for useful discussions in deriving stellar masses. We appreciate the anonymous referee for the comments which improved this paper. The preparation of the observation was in part carried out on "sb" computer system operated by the Astronomical Data Analysis Center (ADAC) and Subaru Telescope of the National Astronomical Observatory of Japan. MA is supported by a Research Fellowship of the Japan Society for the Promotion of Science for Young Scientists. KO is supported by a Grant-in-Aid for Scientific Research from Japan Society for the Promotion of Science (17540216). This work is supported by the Grant-in-Aid for the 21st Century COE "Center for Diversity and Universality in Physics" from the MEXT of Japan.

³ The metallicity of galaxies at $z \sim 2$ (Erb et al. 2006) was derived from N2 index (e.g., Pettini & Pagel 2004) which is different from methods used by Tremonti et al. (2004) and Savaglio et al. (2005) and may have a problems in calibration (e.g., Erb et al. 2006) which may partly be a cause for the offset.

⁴ The stellar masses by Erb et al. (2006) were derived by using Chabrier IMF. Thus our data points should be ~ 1.8 times smaller (e.g., Erb et al. 2006) in Figure 5 in order to compare them with the data by Erb et al. (2006).

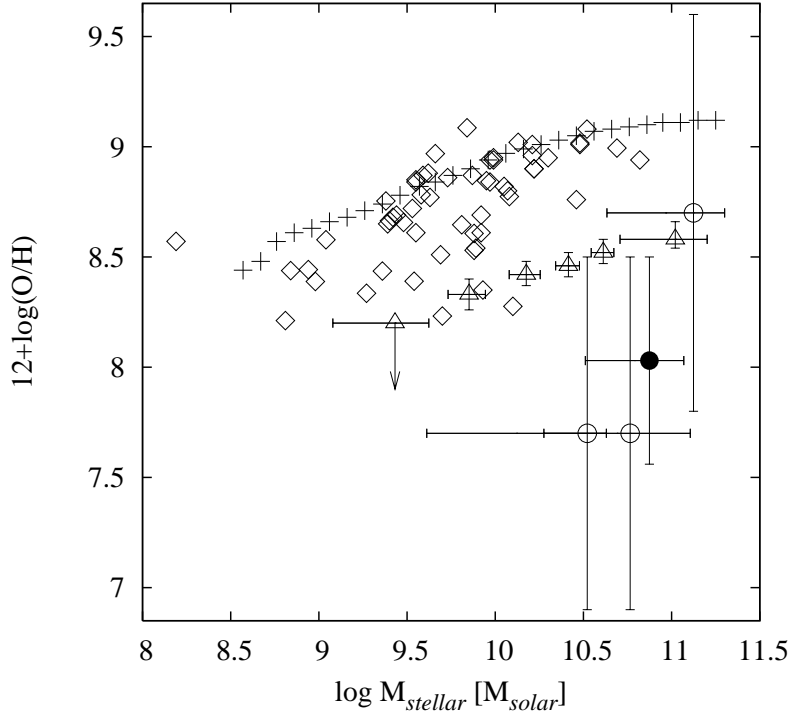


Fig. 5. Stellar mass-metallicity relation for galaxies at various redshifts. Open circles represent our results of 3 luminous LBGs at $z \sim 5$, and filled circle represents the average value of them. Pluses, diamonds, and triangles show the results for galaxies at $z \sim 0.1$, $z \sim 0.7$ and $z \sim 2$, respectively (Tremonti et al. 2004; Savaglio et al. 2005; Erb et al. 2006).

References

- Asplund, M., Grevesse, N., Sauval, A. J., Allende Prieto, C., & Kiselman, D. 2004, *A&A*, 417, 751
- Ando, M., Ohta, K., Iwata, I., Watanabe, C., Tamura, N., Akiyama, M., & Aoki, K. 2004, *ApJ*, 610, 635 (Paper I)
- Ando, M., Ohta, K., Iwata, I., Akiyama, M., Aoki, K., & Tamura, N. 2006, *ApJ*, 645, L9
- Bertin, E., & Arnouts, S. 1996, *A&AS*, 117, 393
- Bouwens, R. J., Illingworth, G.D., Thompson, R. I., & Franx, M. 2005, *ApJ*, 624, L5
- Bouwens, R. J., Illingworth, G.D., Blakeslee, J. P., & Franx, M. 2006, *ApJ*, 653, 53
- Bouwens, R. J., & Illingworth, G.D. 2006, *Nature*, 443, 189
- Calzetti, D., Armus, L., Bohlin, R. C., Kinney, A. L., Koornneef, J., & Storchi-Bergmann, T. 2000, *ApJ*, 533, 682
- Coleman, G. D., Wu, C.-C., & Weedman, D. W. 1980, *ApJS*, 43, 393
- Dey, A., Spinrad, H., Stern, D., Graham, J. R., & Chaffee, F. H. 1998, *ApJ*, 498, L93
- Dickinson, M., et al. 2004, *ApJ*, 600, L99
- Dow-Hygelund, C. C., et al. 2005, *ApJ*, 630, L137
- Erb, D. K., Shapley, A. E., Pettini, M., Steidel, C. C., Reddy, N. A., & Adelberger, K. L. 2006, *ApJ*, 644, 813

- Fioc, M., & Rocca-Volmerange, B. 1997, *A&A*, 326, 950
- Frye, B., Broadhurst, T., & Benitez, N. 2002, *ApJ*, 568, 558
- Heckman, T. M., Robert, C., Leitherer, C., Garnett, D. R., & van der Rydt, F. 1998, *ApJ*, 503, 646
- Inoue, A. K., Iwata, I., Deharveng, J.-M., & Burgarella, D. 2005, *A&A*, 435, 471
- Iwata, I., Ohta, K., Tamura, N., Ando, M., Wada, S., Watanabe, C., Akiyama, M., & Aoki, K. 2003, *PASJ*, 55, 415
- Iwata, I., Inoue, A. K., & Burgarella, D. 2005, *A&A*, 440, 881
- Iwata, I., Ohta, K., Tamura, N., Akiyama, M., Aoki, K., Ando, M., Kiuchi, G., & Sawicki, M. 2007, *MNRAS*, 376, 1557
- Iye, M., et al. 2004, *PASJ*, 56, 381
- Kashikawa, N., et al. 2002, *PASJ*, 54, 819
- Keel, W. C. 2006, *AJ*, 131, 2755
- Kneib, J.-P., Ellis, R. S., Santos, M. R., & Richard, J. 2004, *ApJ*, 607, 697
- Kobulnicky, H. A., & Koo, D. C. 2000, *ApJ*, 545, 712
- Kobulnicky, H. A., & Kewley, L. J. 2004, *ApJ*, 617, 261
- Le Fèvre, O., et al. 2005, *A&A*, 439, L845
- Lehnert, M. D., & Bremer, M. 2003, *ApJ*, 593, 630
- Mannucci, F., Buttery, H., Maiolino, R., Marconi, A., & Pozzetti, L. 2007, *A&A*, 461, 423
- Mehlert, D., et al. 2002, *A&A*, 393, 809
- Miyazaki, S., et al. 2002, *PASJ*, 54, 833
- Noll, S., et al. 2004, *A&A*, 418, 885
- Oke, J. B., & Korycansky, D. G. 1982, *ApJ*, 255, 11
- Oke, J. B., & Gunn, J. E. 1983, *ApJ*, 266, 713
- Ouchi, M., et al. 2004, *ApJ*, 611, 660
- Pello, R., Schaerer, D., Richard, J., Le Borgne, J.-F., & Kneib, J.-P. 2004, *A&A*, 416, L35
- Pettini, M., Shapley, A. E., Steidel, C. C., Cuby, J. G., Dickinson, M., Moorwood, A. F. M., Adelberger, K. L., & Giavalisco, M. 2001, *ApJ*, 554, 981
- Pettini, M., & Pagel, B. E. J. 2004, *MNRAS*, 348, L59
- Pickles, A.J. 1998, *PASP*, 110, 863
- Rix, S. A., Pettini, M., Leitherer, C., Bresolin, F., Kudritzki, R.-P., & Steidel, C. C. 2004, *ApJ*, 615, 98
- Salpeter, E. E. 1955, *ApJ*, 121, 161
- Savaglio, S., et al. 2005, *ApJ*, 635, 260
- Shapley, A. E., Steidel, C. C., Pettini, M., & Adelberger, K. L. 2003, *ApJ*, 588, 65
- Shapley, A. E., Erb, D. K., Pettini, M., Steidel, C. C., & Adelberger, K. L. 2004, *ApJ*, 612, 108
- Shapley, A. E., Steidel, C. C., Pettini, M., Adelberger, K. L., & Erb, D. K. 2006, *ApJ*, 651, 688
- Shimasaku, K., Ouchi, M., Furusawa, H., Yoshida, M., Kashikawa, N., & Okamura, S. 2005, *PASJ*, 57, 447
- Songaila, A., & Cowie, L. L. 2002, *AJ*, 123, 2183
- Songaila, A. 2004, *AJ*, 127, 2598
- Spinrad, H., et al. 1998, *AJ*, 116, 2617

- Stanway, E. R., Bunker, A. J., & McMahon, R. G. 2003, MNRAS, 342, 439
- Stanway, E., Bunker, A., McMahon, R., Ellis, R. S., Treu, T., & McCarthy, P. J. 2004, ApJ, 607, 704
- Steidel, C. C., Giavalisco, M., Dickinson, M., & Adelberger, K. L. 1996, AJ, 112, 352
- Steidel, C. C., Adelberger, K. L., Shapley, A. E., Pettini, M., Dickinson, M., & Giavalisco, M. 2003, ApJ, 592, 728
- Steidel, C. C., Shapley, A. E., Pettini, M., Adelberger, K. L., Erb, D. K., Reddy, N. A., & Hunt, M. P. 2004, ApJ, 604, 534
- Teplitz, H. I., et al. 2000, ApJ, 533, L65
- Tremonti, C. A., et al. 2004, ApJ, 613, 898
- Vanzella, E., et al. 2006, A&A, 454, 423
- Vanzella, E., et al. 2007, Proceedings for the conference "At the Edge of the Universe: Latest results from the deepest astronomical surveys", (astro-ph/0612182)
- Weymann, R. J., Stern, D., Bunker, A., Spinrad, H., Chaffee, F. H., Thompson, R. I., & Storrie-Lombardi, L. J. 1998, ApJ, 505, L95
- Yan, H., et al. 2005, ApJ, 634, 109
- Yoshida, M., et al. 2006, ApJ, 653, 988